

Phase transition characteristics of (Ge₄Sb₄Te₆) thin films using high resolution transmission electron microscope and optical properties

Z. S. El Mandouh⁽¹⁾, H. A. Zayed⁽²⁾, A. H. Hammad⁽¹⁾, Ahmed. R. Wassel^{(1)*}

⁽¹⁾ Thin Films & Electron Microscope Department, Physics Division, National Research Center, Dokki, 12311 Cairo, Egypt.

⁽²⁾ Physics Department, Faculty of Girls, Ain-Shams University, Cairo, Egypt.

Abstract: Thin amorphous films of (Ge₄Sb₄Te₆) have been widely employed in the technology. It has been prepared on glass substrates by a thermal evaporation technique. The target materials used for the films deposition were prepared by conventional solid state reaction in a vacuum sealed silica tube to avoid oxide formation. The effect of thermal annealing on structure and optical properties had been investigated. As deposited and annealed films from 200°C to 350°C was investigated by X-ray diffraction (XRD), and high resolution transmission electron microscope (HRTEM). The optical constants were determined from the spectrophotometric measurements of the transmittance and reflectance spectra. The optical absorption coefficient was analyzed to identify the type of the optical transition and for determination of band gap values. (XRD) and (HRTEM) results show that amorphous to crystalline phase transition occur after annealing and the crystallinity degree increases with increasing annealing temperature. Used for phase change optical memory or compact disks.

Keywords: Thin films-thermal annealing-amorphous-crystalline.

I. Introduction

Chalcogenide glasses are widely used for a variety of application such as optical memory, fiber optics, and device for data storage as well as non volatile electronic storage. It should be noticed that such materials endorse an amorphous to crystalline phase transition with electrical switching property which constitute an advantageous features suitable for various industrial applications [1-5]. Many investigations have been carried out on Se-Te system with the aim of improving its properties and versatility. It is worth mentioning that the past decades have seen a spate of research efforts and numerous doping element were tried [6-11], but often it is rather difficult choose appropriate elements that could positively influence Se-Te system. Elemental Ge is considered to be effective in forming covalent bonds and reducing the atomic diffusivity which can provide sufficient amorphous stability [12]. Alloys containing Ge element are receiving the greatest attention in the nonvolatile memory device application called phase change random accesses memory (PCRAM) especially for (Ge₂Sb₂Te₅) based material systems [13-15]. Now days Ge-Sb-Te chalcogenide, which undergo phase transformations under the action of external stimuli, are of tremendous technological importance ranging from optical data storage to phase-change random access memory (PRAM), exhibiting the best performance for DVD-RAM in terms of speed and stability, Ge₂Sb₂Te₅ (hereafter GST) is also currently the most focused phase-change alloy [16-18]. The structure, optical and electrical properties of the chalcogenide are well known. There exist three solid phases in GST: amorphous, metastable rocksalt (face-centered-cubic, FCC) and stable hexagonal (Hex) phases. The whole switching operation in optical data storage and electronic memories is based on the following rapid cycling processes by either laser or electric heating: amorphous → FCC (Erase/SET process) → Hex → liquid → amorphous (Write/RESET process) [19, 20]. In this study, the Ge-Sb-Te phase change recording films were prepared by thermal evaporation technique. The dependence of structure and optical parameters on annealing temperature was investigated.

II. Materials And Methods

Bulk compositions of (Ge₄Sb₄Te₆) alloys were prepared by melt quenching technique. The constituent elements (99.999% purity) were weighted according to their atomic percentage (at.%) and were sealed in a quartz ampoule (length ~10 cm, and diameter ~6 mm), in a vacuum of ~10⁻³ mbar. The sealed ampoule was kept in a furnace for 24h and the temperature was raised to 1000 °C, at a rate of 4-5°C/min. The ampoule was rocked constantly to ensure homogeneous mixing of the melt. Finally, the ampoule containing molten alloy was quenched in ice-cold water. The bulk material was extracted from quartz ampoule. Ingot so obtained was crushed into fine powder. Thin films of the above-mentioned Ge₄Sb₄Te₆ alloys were prepared by thermal evaporation method using An Edward- coating unit (EDWARDS E306). X-rays diffraction was carried out on

both powder and films forms using (X'Pert Pro (PANalytical)) operating at with Target Cu-K_α radiation with secondary monochromatic, operating at power= 45 kV and current equal 40 mA (Holland). The diffraction data was recorded for 2θ values between 4° and 70° and the scanning rate was (10°/min). A double beam UV–VIS–NIR, V-578) was used at normal light incidence to record the optical transmission and reflection spectra of the deposited films over the wavelength range 500–2500 nm. All the measurements were made at room temperature, and a very good reproducibility of the spectra was generally achieved. The morphology and structure of thin films samples were studied by high resolution transmission electron microscope (HRTEM) (JEM-2100) Jeol.

III. Results And Discussion

1. X-ray analysis.

The X-ray diffraction study leads to detection of the amorphous state and several crystalline phases. The (XRD) patterns of the composition (Ge₄Sb₄Te₆) for as deposited and annealing temperatures are shown in **figure (1.1)**. The absence of any sharp peaks in as deposited film confirm the amorphous state, and the existence of sharp peaks in annealing temperatures films indicate the polycrystalline behavior of thin films. It has been observed in the chart of XRD, transition from amorphous state to face center cubic (FCC) structure and transform from (FCC) Phase to Hexagonal phase at higher temperatures. The intensity of peaks and the angle of diffraction (2θ) show the planes and the orientation for crystalline films. In face centered cubic structure, these planes are (111), (200), (220), and (222) corresponding to angles (2θ) (25.7°), (28.5°), (42.5°), and (53.21°). On the other hand, in the hexagonal structure, these planes are (005), or (103), (200), (220) or (210), and (222). All these data as confirmed by (JCPDS database 1998). We found there exist three solid phases in (GST), amorphous, metastable rock salt structure (face centered cubic FCC structure) and stable hexagonal phase. It was confirmed by **Weidenhof et al.** that (Ge₂Sb₂Te₅) films annealed at 200°C for 30 min lead to the formation of metastable rock salt structure [21]. The stable hexagonal phase was reported to consist of cycling nine layers in one unit cell, e.g., -Te-Ge-Te-Sb-Te-Te-Sb-Te-Ge- stacking order. While the FCC structure has six layers stacking and the hexagonal structure has nine layers stacking [22, 23].

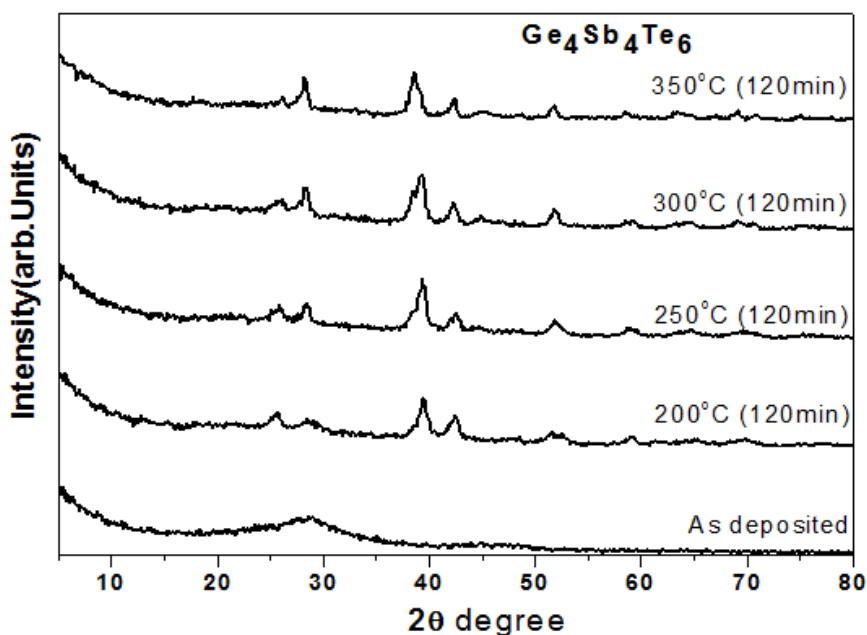


Figure (1.1) X-Ray diffraction patterns of as deposited and annealed film of Ge₄Sb₄Te₆.

2. Determination of Crystal Size of Thin Films

The Average size (D) of the crystalline grains of thin films can be evaluated by (Debey- Scherrer's formula) [24].

$$D = \frac{0.9 \lambda}{\beta \cos \theta} \quad (1.1)$$

Here, (λ) Wave length of X-ray (λ=0.1541 nm).

(β) Full-width at half maximum (FWHM) of peaks intensity.

(θ) Bragg angle.

The calculated grain size is varied from (13.4 nm) to (19.5 nm) with annealing due to variation in corresponding (FWHM) as represented in **table (1.1)**, and **Figure (1.2)**. It can be seen that the crystal size depends on the annealing temperatures. In the composition (Ge₄Sb₄Te₆), the crystal size increased as temperatures is increased from 200°C and 350°C which may be due to coalescence or aggregation of small nanocrystalline particles, there is an odd behavior was observed at 250°C, that the crystal size was increased[25, 26].

Table (1.1). The values of crystal size for (Ge₄Sb₄Te₆) thin films.

<i>Crystal Size for(Ge₄Sb₄Te₆)</i>			
At 200°C	At 250°C	At 300°C	At 350°C
13.4075nm	19.50031nm	15.3197 nm	17.8273 nm

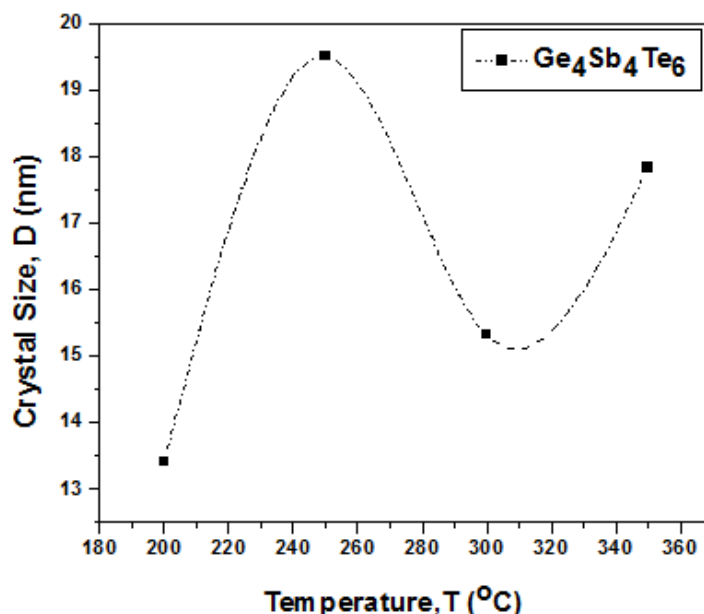


Figure (1.2) crystal size with annealing temperature of (Ge₄Sb₄Te₆) thin films

3. Microstructure of (Ge₄Sb₄Te₆) thin films

The microstructure of Ge₄Sb₄Te₆ thin films investigated by high resolution transmission electron microscope (HRTEM) to indicate the change from amorphous state to crystalline state. **Figure (1.3)** shows (HRTEM) and selected area electron diffraction patterns for as deposited and different annealed films. The HRTEM images of as deposited films for this composition, exhibits a uniform contrast and featureless topography indicating an amorphous structure. This structure is confirmed by the halo diffraction rings. Increasing temperature; a well defined crystals observed with cubic projection indicating crystallization as confirmed by electron diffraction. The phase is one of two crystalline phases of Ge-Sb-Te, Yamada proposed that metastable face centered cubic was rocksalt structure with space group Fm-3m [27, 28]. While Kolobov et al. proposed that during the phase transformation of GeSbTe from amorphous to the metastable structure, an umbrella flip of Ge-atoms from a tetrahedral position into an octahedral position occurs which leads to the fast crystallization of GeSbTe [29]. Increasing annealing temperature to 250°C, particle size was increased due to coalescence and well defined electron diffraction. Electron diffraction shows the formation of stable hexagonal phase. Increasing the annealing temperature to 300°C leading to growth of fine grain and the crystal size gets smaller. Further increase of temperature to 350°C leads to coalescence to bigger particles with distorted out lines.

4. Lattice structure

HRTEM images and Fourier transform image of GST annealed thin films was observed in **figure (1.4)**. HRTEM images clearly show the crystallinity of GST thin films according to the annealing temperatures. The Fourier transform images obtained with HRTEM show the crystal structure of GST.

- At 200°C image (1.4) shows the coexistence of metastable cubic phase and amorphous phase.
- At 250°C, a hexagonal phase was observed coexist with cubic phase.
- At 300°C, a hexagonal phase manifests itself.
- At 350°C, change of orientation was observed.

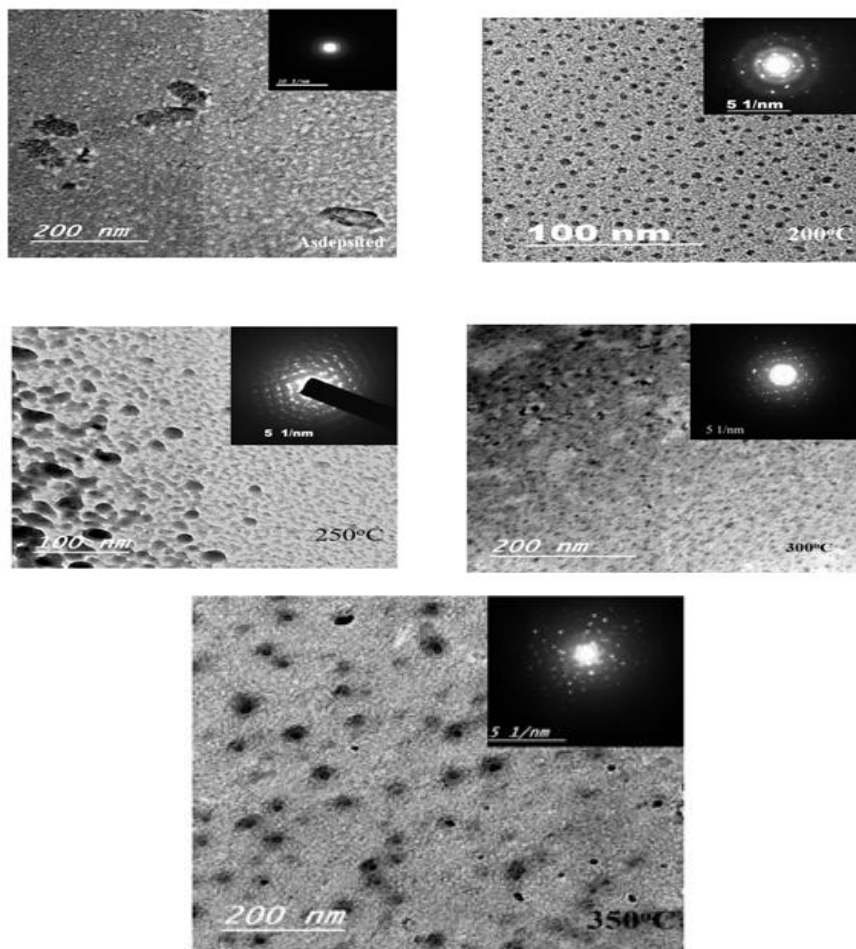


Figure (1.3) Microstructure for Ge₄Sb₄Te₆ thin film

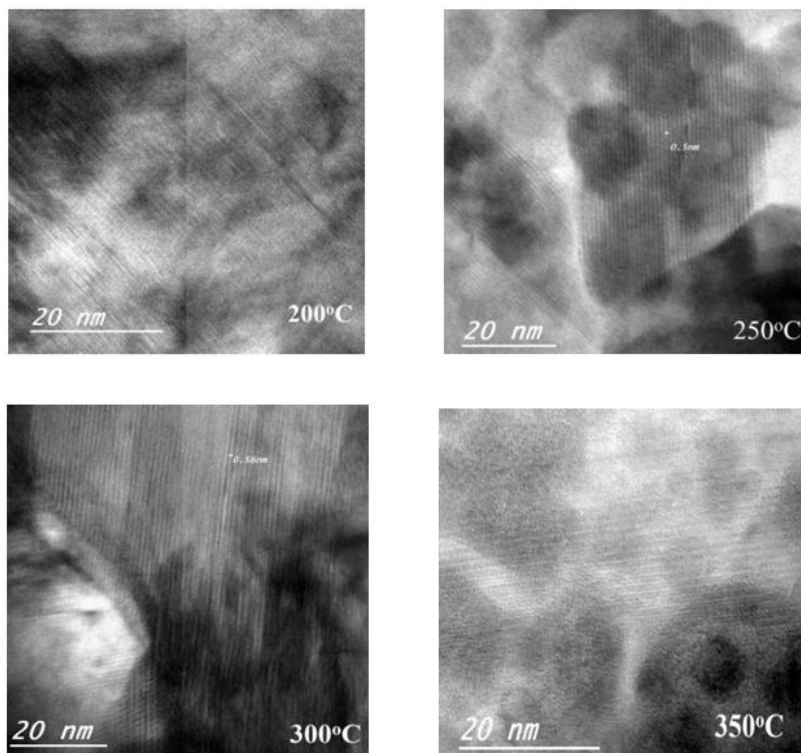


Figure (1.4) lattice structure for Ge₄Sb₄Te₆ thin film

IV. Optical Properties For $\text{Ge}_4\text{Sb}_4\text{Te}_x$ Thin Films

4.1 Transmittance and reflectance

The transmittance, T and reflectance R spectra of the as-deposited and annealed films for the composition of $\text{Ge}_4\text{Sb}_4\text{Te}_6$ as a function of the wavelength ranging from 500 to 2500 nm are presented in the **figure (1.5), and figure (1.6)**. When the thin film samples heated at different temperature, the transmittance is observed to decrease to low values, in this composition thin film, the transmittance is sharply dropped from about 0.31 to 0.095 when heated to 200 °C. By increasing the temperature from 200 to 350 °C, the transmittance is observed to slightly increase but at low value to reach 0.115. Also, when the annealing temperature is increased, the absorption edges of these films shift toward the longer wavelengths and the magnitude of the absorption edge decreases as the annealing temperature increases. In contrast to crystalline semiconductors the optical absorption edge of amorphous semiconductors does not terminate abruptly at the band edge. The existence of tail states in amorphous semiconductors induces a profound impact upon the band to band optical transitions. There is often a wide variation in the sharpness of the edge for the same material when subjected to annealing [30]. This behavior may be attributed to the increasing crystallinity of the film, which is proportional to the scattering loss [31].

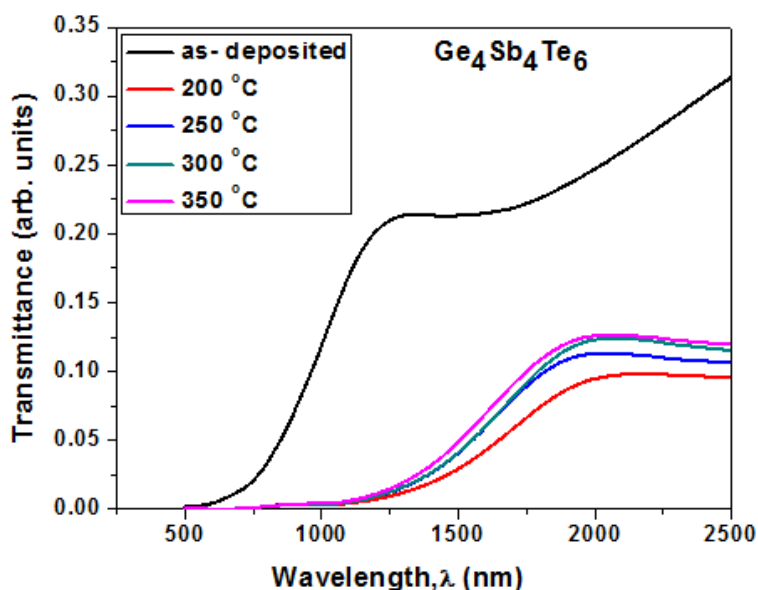


Figure (1.5) Transmittance spectra of $\text{Ge}_4\text{Sb}_4\text{Te}_6$ films

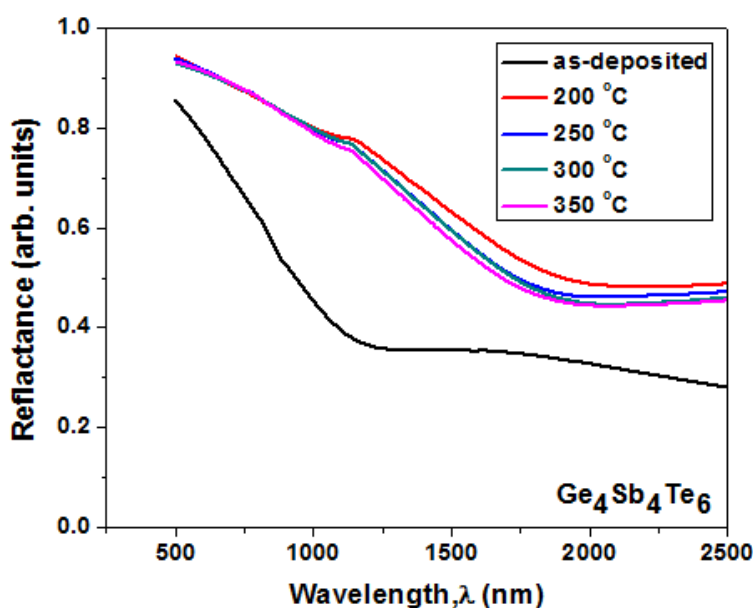


Figure (1.6) Reflectance spectra of $\text{Ge}_4\text{Sb}_4\text{Te}_6$ films

4.2. Absorption coefficient of Ge₄Sb₄Te₆ thin films

Optical constants of the as-deposited and annealing films were studied. The dependence of the absorption coefficient on the photon energy has been calculated from equation (1.2). The absorption coefficient, α was determined from the relation:

$$\alpha = \frac{1}{d} \ln \left(\frac{I_0}{I} \right) \quad (1.2)$$

Where I_0/I is the transmittance ratio and d is the film thickness in units of centimeter. For higher values of α ($\alpha > 10^4 \text{ cm}^{-1}$) where the absorption is associated with inter band transitions which obeys the Tauc law [32].

In the absorption process, the photon of known energy excites an electron from the lower to the higher energy state corresponding to the absorption edge. In chalcogenide glasses, a typical absorption edge can be broadly ascribed by any of the following processes:

- i. Residual below-gap absorption.
- ii. Urbach tails.
- iii. Inter band absorption at high energy.

Chalcogenide glasses were found to exhibit highly reproducible optical edges, which are relatively insensitive to the preparation conditions and only the observable absorption with a gap under equilibrium conditions account for the first process [33]. In the second process the absorption edge depends exponentially on the photon energy according to the Urbach relation [34]. In the crystalline materials, the fundamental edge is directly related to the conduction band and valence band, i.e. direct and indirect band gaps, while in the case of amorphous materials the optical transition is different. This behavior has also been observed in many chalcogenide [35]. In the present work, it has been observed that the values of α is decreasing exponentially with increasing the wave length, and the curves of α exhibit a characteristic feature that the value of α is high ($\alpha=5 \cdot 10^4$ to $5 \cdot 10^5$) which is the case for highest carrier concentration semiconductor. It was observed that as deposited films have the lowest value of (α), also increases with increasing the temperature from (200-350 °C) as shown in figure (1.7).

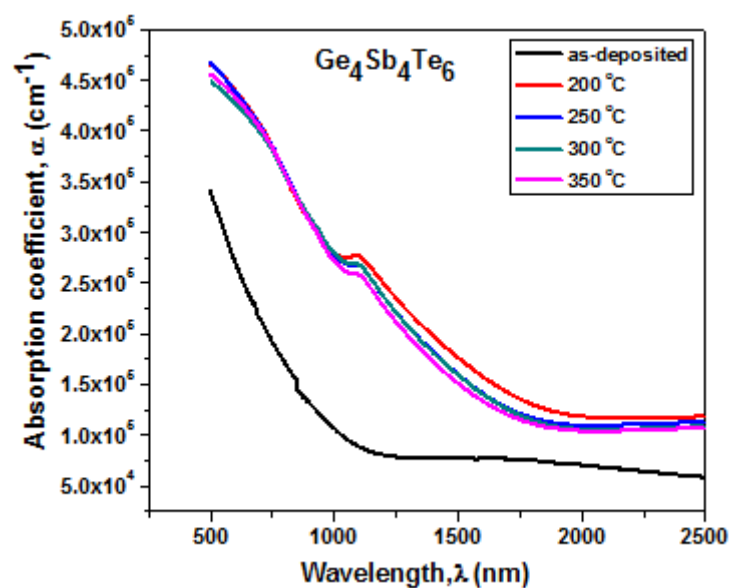


Figure (1.7) Absorption coefficient spectra of Ge₄Sb₄Te₆ films

4.3 Optical band gap and Urbach energy.

Generally, semiconductors and insulators have a fundamental absorption edge in the near infrared, visible, or ultraviolet spectral region. The absorption edge is due to the onset of optical transitions across the fundamental band gap of the material. This naturally leads us to investigate the physical processes that occur when electrons are excited between the bands of a solid by making optical transitions [36].

For amorphous materials the optical absorption at a higher value of α (ν) greater than (10^4 cm^{-1}) above the exponential tail follows a power law given by Davis and Mott [37], which is the most general form given:

$$\alpha = B \frac{(h\nu - E_g)^r}{h\nu} \quad (1.3)$$

where (r) is an index that can have different values: 2, 3, 1/2 and 1/3 corresponding to indirect allowed, indirect forbidden, direct allowed and direct forbidden transitions, respectively. (B) is a constant called band tailing parameter, (E_g) is the optical band gap energy and ($h\nu$) is the incident photon energy. Using **equation (1.3)**, a plot is drawn between $(\alpha h\nu)^{1/2}$ and $(\alpha h\nu)^2$ as function of photon energy ($h\nu$) as shown in **figure (1.8)**, and **figure (1.9)**, from the graph one can find the optical energy band gap for direct and indirect allowed transitions. The respective value of (E_g) is obtained by extrapolating the linear region of the curve to the $h\nu$ axis where $(\alpha h\nu)^{1/r} = 0$ for both transition cases and the values are listed in the Table (1.2) for thin film as deposited and annealed thin films.

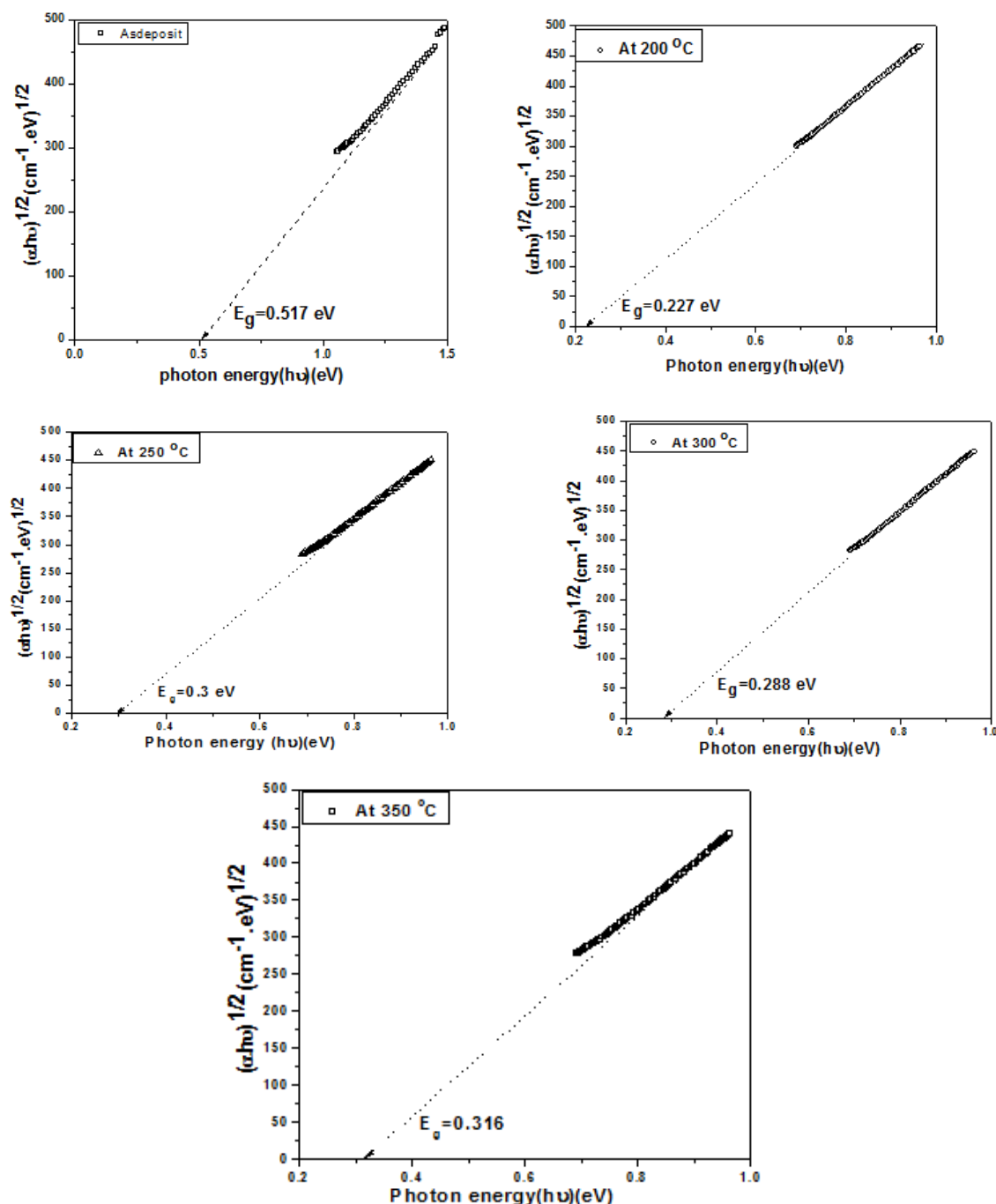


Figure (1.8) indirect optical band gap as a function of photon energy for $(\text{Ge}_4\text{Sb}_4\text{Te}_6)$ as deposited and annealed thin films.

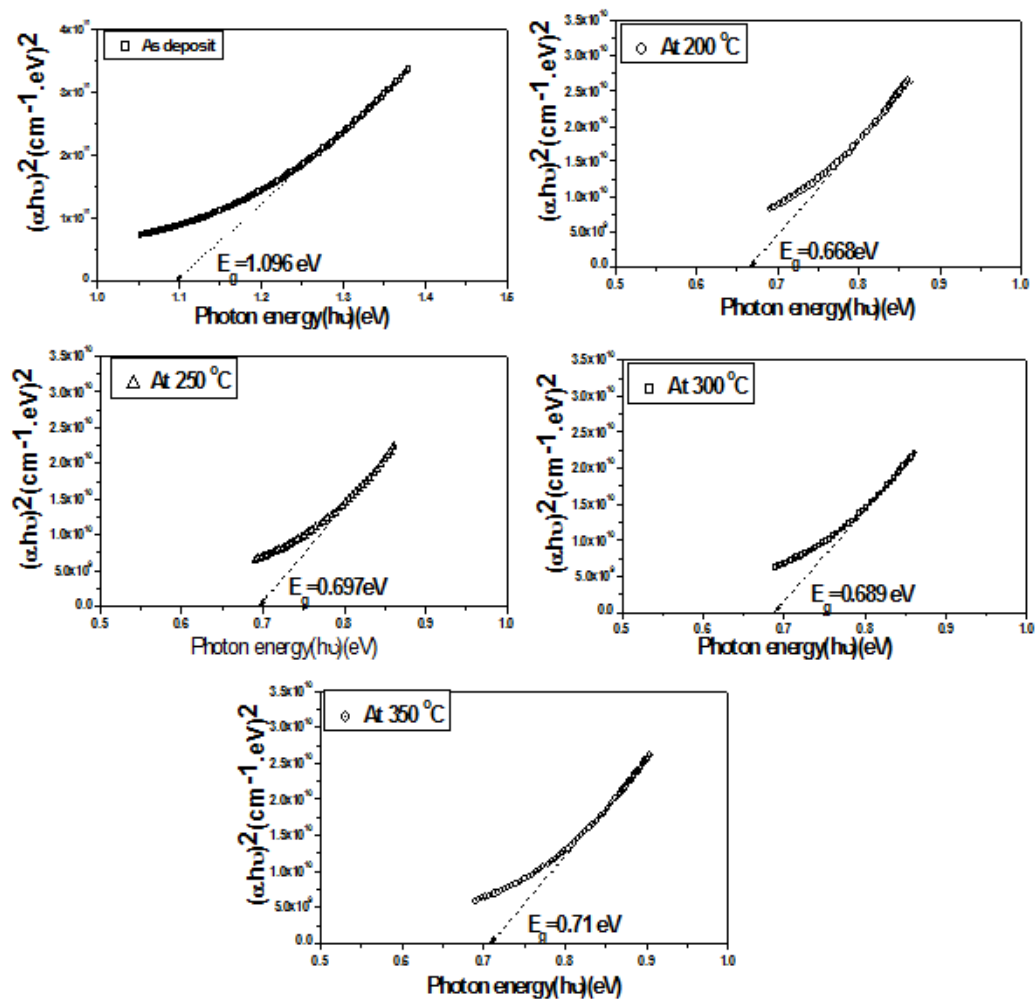


Figure (1.9) direct optical band gap as a function of photon energy for $(\text{Ge}_4\text{Sb}_4\text{Te}_6)$ as deposited and annealed thin films.

Table (1.2) indirect & direct optical energy gap for composition $\text{Ge}_4\text{Sb}_4\text{Te}_6$

Indirect band gap energy, $^{indi}E_g$ (eV)		direct band gap energy, $^{di}E_g$ (eV)
$\text{Ge}_4\text{Sb}_4\text{Te}_6$		$\text{Ge}_4\text{Sb}_4\text{Te}_6$
As deposited	0.517	1.096
200 ° C	0.227	0.668
250 ° C	0.3	0.697
300 ° C	0.288	0.689
350 ° C	0.316	0.71

The observed decrease of optical gap for $\text{Ge}_4\text{Sb}_4\text{Te}_6$ films with annealing temperature in **table 1.2** can be explained according to Hesegawa et al. [38, 39] suggestion; they suggested that the unsaturated bonds are responsible for the formation of localized tail states in the band gap. The presence of a high concentration of these states is responsible for the decrease of (E_g) in the deposited films. The drastic effect of annealing (crystallization) on optical gap can be explained as a result of the production of surface dangling bonds, further increasing of annealing temperature results in the breaking up of the formed crystallites into smaller crystallites, thereby increasing the number of surface dangling bonds responsible for the formation of some types of defects. These defects lead to the decrease of the optical gap [34]. During heat treatment, the defects are gradually annealed out of producing larger number of saturated bonds. The reduction in the number of unsaturated defects decreases the density of localized states in the band structure and consequently increases the optical gap to a steady value. Effect of annealing temperature on direct and indirect energy gap was illustrated in **figure (1.10)**. It is clear from the figure; that the indirect and direct energy gaps reduce with increasing annealing temperatures and reaches a steady value at high temperature.

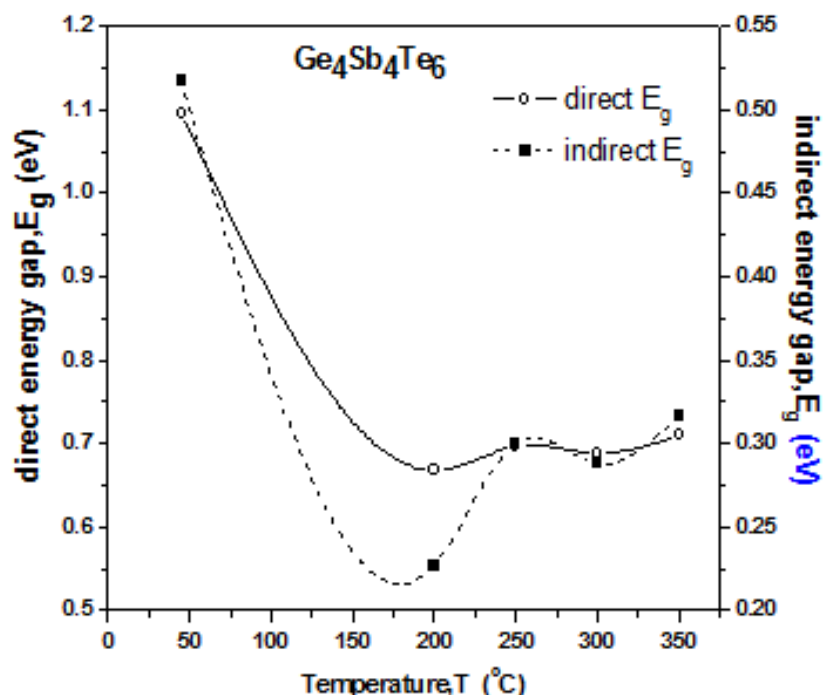


Figure (1.10) the variation of direct & indirect optical band gap as a function of Temperature for (Ge₄Sb₄Te₆) thin film.

In amorphous materials there exists a band tailing in the forbidden energy band gap. The extent of band tailing is a measure of the disorder in the material and can be estimated by using the Urbach Equation (1.4). The band tails width of localized states (ΔE) near the band edges can be calculated using Urbach empirical relation [40]:

$$\alpha = \alpha_0 \exp\left(\frac{h\nu}{\Delta E}\right) \quad (1.4)$$

Where (α_0) is a constant, ($h\nu$) is incident photon energy, and (ΔE) is the Urbach energy interpreted as the width of the tail of localized states in the normally forbidden band gap, which are associated with the amorphous nature. Figure (1.11), represent the relationship between $\ln(\alpha)$ and $h\nu$ to find the values of the Urbach energy. ΔE can be calculated from the reciprocal of the slope of the linear region of such plots and the data are listed in Table (1.3). Conduction band tailing is known to occur in disordered materials which result in a reduction of the optical gap energy. In structurally disordered films the imperfection in the film causes the bonds of localized states to get broaden and a band gap reduction may occur due to Urbach energy. **Ananth et al. [41]** reports that from Urbach energy the structural disorder is addressed as the basis of band tailing due to the creation of localized energy states. While **Yong Wang et al. [42]** indicates that materials with larger Urbach energy have a greater tendency to convert weak bonds (homo polar bond such as Ge-Ge, Te-Te) into defect and will increase disorder.

Table (3.1) Urbach energy data for (Ge₄Sb₄Te₆) thin films as deposited and annealed thin films.

Urbach energy, ΔE (eV)	
Ge ₄ Sb ₄ Te ₆	
As deposited	0.635
200 °C	0.502
250 °C	0.464
300 °C	0.462
350 °C	0.463

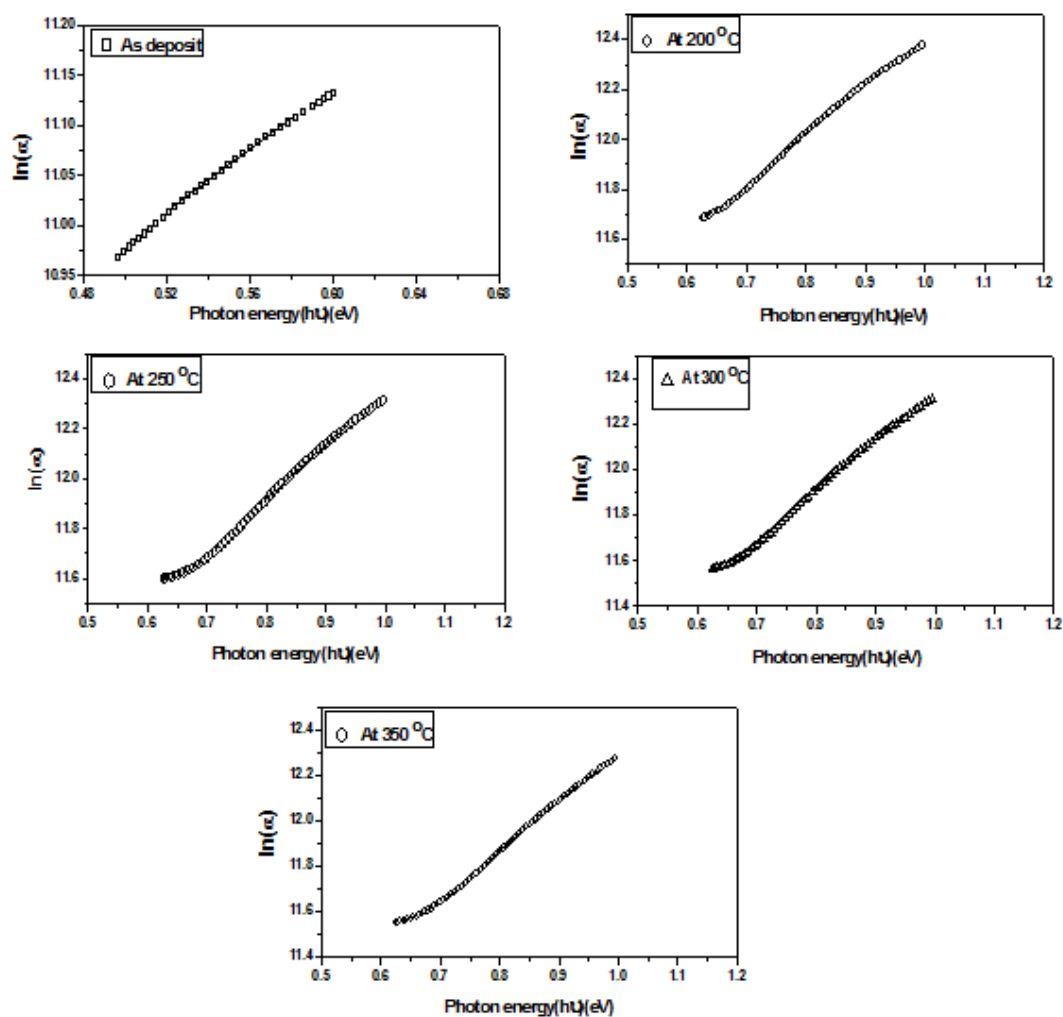


Figure (1.11) Variation of $\ln(\alpha)$ as a function of the photon energy for $(\text{Ge}_4\text{Sb}_4\text{Te}_6)$ thin films at different annealing temperature

V. Conclusion

We investigated the effects of addition of (Te) and temperature on the phase change behavior and microstructure of $\text{Ge}_4\text{Sb}_4\text{Te}_6$.

- 1- X ray diffraction show the change of GST from amorphous to face centered cubic (metastable phase) and then to stable hexagonal phase at high temperature.
- 2- Lattice pattern confirm the transformation from amorphous to crystalline.
- 3- From transmittance and reflection data direct and indirect optical energy gap was calculated, and they decrease as temperature increases which is attributed to the production of surface dangling bonds which are responsible of formation of localized tail states in the band gap.
- 4- Urbach energy was calculated which is a measure of disorder, larger Urbach energy larger disorder.

References

- [1]. E. Morales-Sanchez, B. Lain, E. Prokhorov, M.A. Hernandez-Landaverde, G. Trapaga, J. Gonzalez-Hernandez, Vacuum 84 (2010) 87781.
- [2]. M. Naito, M. Ishimaru, Y. Hirotsu, R. Kojima, N. Yamada, J. Appl. Phys. 107 (2010) 103507.
- [3]. I.A. Mahdy, E.P. Domashevskaya, P.V. Seredin, O.B. Yatsenko, Opt. Laser Technol. 43 (2011) 20.
- [4]. A. Shamshad, M. Khan, M. Zulfequar, M. Husain, Physica B 324 (2002) 336.
- [5]. A. Mendoza-Galvana, E. Garcia-Garciab, Y.V. Vorobieva, J. Gonzalez-Hernandez, Microelectron. Eng. 51–52 (2000) 677.
- [6]. V. Sharma, A. Thakur, N. Goyal, G.S.S. Saini, S.K. Tripathi, Semicond.Sci. Technol. 20 (2005) 103.
- [7]. A. Sharma, P.B. Barman, Thin Solid Films 517 (2009) 3020.
- [8]. K.A. Aly, J. Non-Cryst. Solids 355 (2009) 1489.
- [9]. E. Chandasree, M.G. Mahesha Das, G. Mohan Rao, S. Asokan, Thin Solid Films 520 (2012) 2278.
- [10]. N.B. Maharjan, K. Singh, N.S. Saxena, Phys. Status Solidi (A) 195(2003) 305–310.
- [11]. V. Pandey, N. Mehta, S.K. Tripathia, A. Kumar, Chalcogenide Lett2 (2005)39.
- [12]. Saleh Saleh Ahmed, Mater. Sci. Appl. 2 (2011) 950–956.
- [13]. S. Lai, IEDM Tech. Dig. (2004) 225.

- [14]. D.Z. Dimitrov, V.-H. Lu, M.R. Tseng, W.C. Hsu, H-P.D. Shieh, Jpn. J. Appl. Phys. 41 (2002) 1656.
- [15]. H.J. Borg, M. Schijndel, J.C.N. Rjpers, M.H.R. Lankhort, G. Zhou, M. J. Dekker, I.P.D. Ubbens, M. Kuijper, Jpn. J. Appl. Phys. 40 (2001)159.
- [16]. Kolobov, A.V. (2008) Information storage: Around the phase-change cycle. Nat. Mater. 7, 351–353.
- [17]. Wuttig, M., Lusebrink, D., Wamwangi, D., Welnic, W., Gillessen, M. & Dronskowski, R. (2007) “the role of vacancies and local distortions in the design of new phase-change materials”. Nat. Mater. 6, 122–127.
- [18]. Sun, Z., Zhou, J. & Ahuja, R. (2007) “unique melting behavior in phase change materials for rewritable data storage”. Phys. Rev. Lett. 98,055505.
- [19]. Song, S.A., Zhang, W., Jeong, H.S., Kim, J.G. & Kim, Y.J. (2008) “In situ dynamic HR-TEM and EELS study on phase transitions of Ge₂Sb₂Te₅ chalcogenides”. Ultramicroscopic 108, 1408–1419.
- [20]. Schreiber, M. (2011) Phase-change materials: Disorder can be good. Nat. Mater. 10, 170–171.
- [21]. V. Weidenhof, I. Friedrich, S. Ziegler, M. Wuttig, J. Appl. Phys. 89 (2001) 3168.
- [22]. B.J. J. Kooi and T. M. De Hosson, J. Appl. Phys. 92, 3584 (2002).
- [23]. T. Matsunaga, N. Yamada, and Y. Kabota, Acta Crystallogr. Sect. B 60, 685(2004).
- [24]. J. Lou and N. Audebrand, "Profile fitting and diffraction line-broadening analysis," Adv. X-ray Anal., vol. 41, pp. 556-565, 1997.
- [25]. T.S. Shyju, S. Anandhi, R. Indirajith, R. Gopalakrishnan, Solvothermal “synthesis,deposition and characterization of cadmium selenide (CdSe) thin films by thermal evaporation technique”, J. Cryst. Growth 337 (2011) 38.
- [26]. N. Revathi, P. Prathap, K.T.R. Reddy, “Thickness dependent physical properties of close space evaporated In₂ S₃ films”, Solid State Sci 11 (2009) 1288.
- [27]. N. Yamada and T. Matsunaga. J. Appl. Phys. 88, 7020(2000).
- [28]. T. Nonaka, G. Ohbayashi, Y. Toriumi, Y. Mori, and H. Hashimoto; Tin Solid Films 370(285) (2000).
- [29]. A. V. Kolobov, P. Fons, A. I. Frenkel, A. L. Ankudinov, J. Tomnaga, and T. Uruga, Nat. Mater. 3,703(2004).
- [30]. G. D. Cody in semiconductors and semi-metals, vol.21, part B edited by J.I. Pankove (Academic Press, Newyork) pp.11 (1984).
- [31]. R.A. Street, R.J. Nemanich, G.A.N. Connell, “Thermally induced effects in evaporated chalcogenide films”. II. Optical absorption, Phys. Rev. B 18 (1978) 6915–6919.
- [32]. J. Tauc, R. Grigorovici, A. Vancu, Phys. Stat. Sol. 15 (1966) 627.
- [33]. J. Tauc, in: J. Tauc (Ed.), Amorphous and Liquid Semiconductors, Plenum Press, London and New York, 1974.
- [34]. F. Urbach, Phys. Rev. 92 (1953) 1324.
- [35]. N.F. Mott, E.A. Davis, Electronic Processes in Non-Crystalline Materials, 2nd edn Clarendon, Oxford, 1979.
- [36]. M. Fox, Ed., Optical Properties of Solids, Oxford University Press Inc., New york, 2001, p. 49.
- [37]. E. A. Davis and N. F. Mott, "Conduction in non-crystalline systems V. Conductivity, optical absorption and photoconductivity in amorphous semiconductors," *Philos. Mag.*, vol. 22, no. 179, pp. 903-922, 1970.
- [38]. S. Hasegawa, S. Yazaki, Solid State Commn. 23(41),(1977).
- [39]. S.Hasegawa, M. Kitagawa, Solid State Commn. 27(855),(1978).
- [40]. S.Choudari, S.K.Biswas, J. of Non-crystalline Solids. 54(179), (1983).
- [41]. R.T. Ananth Kumar, P. Chithra Lekha, C. Sanjeevirasa, D.P. Athinettam Padiyan, J. of Non-crystalline Solids. 504, (PP.21-26), (2014).
- [42]. Yong Wang, Kouhei Tanaka, Kazuo Murase, Physica B316-317,pp.568-571,(2002).